MASTER THESIS

MACHINE LEARNING FOR INTENT RECOGNITION IN A POWERED KNEE PROSTHESIS

S.H.G. Nies

FACULTY OF ENGINEERING TECHNOLOGY
DEPARTMENT OF BIOMECHANICAL ENGINEERING

EXAMINATION COMMITTEE
PROF. DR. IR. HERMAN VAN DER KOOIJ
DR. IR. RENÉ FLUIT
DR. IR. JAN DE JONG

DOCUMENT NUMBER
BW - 721

UNIVERSITY OF TWENTE.

13-05-2020

SAMENVATTING

Doel: Het ontwikkelen van een support vector machine (SVM) voor een actieve knieprothese om overgangen tussen bewegingsmodi te voorspellen: intentieherkenning. De onderzochte bewegingsmodi zijn lopen op een vlakke ondergrond en traplopen. Daarnaast wordt ook de meerwaarde van proefpersoonspecifieke SVM's onderzocht. Een proefpersoonspecifieke SVM houdt in dat alleen de data van die specifieke proefpersoon wordt gebruikt om te voorspellen of hij of zij gaat veranderen van bewegingsmodus. Het is van belang dat deze overgangen op een veilige manier plaatsvinden, zodat de gebruiker niet verstoord wordt in zijn balans. Daarnaast is het ook belangrijk dat de voorspelling nauwkeurig is, zodat de prothese niet op onverwachte manieren beweegt.

Methode: Van drie proefpersonen is data verzameld tijdens het lopen, traplopen en overgangen hiertussen. Deze data gaven informatie over de positie en oriëntatie van de gewrichten en de krachten die er op de prothese spelen. Er wordt geanalyseerd wanneer de beslissing om van bewegingsmodus te veranderen gemaakt had moeten worden om een soepele overgang te kunnen uitvoeren. Het effect van aanpassingen in de input data voor de SVM op de nauwkeurigheid van de voorspellingen is geanalyseerd op drie aspecten: het aantal geanalyseerde proefpersonen, het deel van de loopcyclus dat bekeken wordt en het aantal klasses waarin de data onderverdeeld wordt. Met het aantal klasses onderverdelen wordt bedoeld of de overgangen en de modi zelf samengevoegd worden in één klasse of dat ze gesplitst worden in twee klasses.

Resultaten: Er zijn kleine onderlinge verschillen in de looppatronen van de verschillende proefpersonen, zoals de tijdsduur per stap. Dit heeft een effect op het optimale tijdstip waarop de overgang tussen bewegingsmodi plaats moet vinden. Ook de fase van de loopcyclus die het beste is om te gebruiken voor de voorspelling hangt af van de proefpersoon.

Conclusie: Proefpersonen vertoonden iets afwijkende bewegingspatronen ten opzichte van elkaar, waardoor het optimale tijdstip persoonsafhankelijk is. Bovendien resulteerde een proefpersoonspecifieke SVM in de hoogste nauwkeurigheid van intentieherkenning. Het scheiden van de data van overgangen tussen modi en de modi zelf verbeterde de nauwkeurigheid van de intentieherkenning nauwelijks.

Relevantie: Deze studie suggereert dat de focus moet liggen op proefpersoonspecifieke SVMs voor het voorspellen van overgangen tussen bewegingsmodi, in plaats van op algemene SVMs die op alle geamputeerden kunnen worden toegepast.

Machine learning for intent recognition in a powered knee prosthesis

S.H.G. Nies, *s.h.g.nies@student.utwente.nl, s1559516, MSc student BME*

***Abstract*—*Objective:* To develop a support vector machine (SVM) to predict locomotion mode transitions between level-ground walking and stair ascent, and to investigate the additional value of subject-specific SVMs. *Methods:* Training data consisted of steady-state level-ground walking and stair ascent, and transitions between them. The effect of input data on the accuracy of the SVM has been analyzed with regard to three aspects: the number of included subjects, the analyzed portion of the gait cycle, and the number of classes. *Results:* Optimal characteristics of the SVM input data, such as the selected portion of the gait cycle, were subject-specific. The number of classes did not strongly affect the accuracy of the prediction. *Conclusion:* Subjects exhibited slightly different locomotion patterns, affecting the optimal timing of the prediction. Furthermore, a subject-specific SVM resulted in the highest accuracy of intent recognition. Separating transitional and steady-state data into two classes hardly improved the intent recognition accuracy. *Significance:* This study suggests that the focus should be on subject-specific models for intent recognition, rather than general models that can be applied to all amputees.**

***Index Terms*—Intention detection, locomotion modes, subject-specific, transfemoral amputee**

I. Introduction

TRANSFEMORAL Microprocessor-controlled Prosthetic Knees (MPKs) are medical devices that restore walking function for transfemoral amputees (TFAs). They mimic the healthy biological knee function and control the movement of the joint on a real-time basis by using sensory information recorded from a variety of sensors, such as an inertial measurement unit (IMU) and a load cell. These sensors give information about the orientation and position of the joint and the applied forces and moments on the MPK, respectively. This can be done by either passive knee prostheses (P-MPKs), which have variable damping, or active prosthetic knees (A-MPKs) which contain a motor. A-MPKs can actively extend the knee and thereby permit the user to execute energy-demanding tasks, such as standing up from a sitting position. Furthermore, they permit additional locomotion modes, such as step-over-step stair ascent. However, the differences between locomotion modes are large. For instance, the knee flexes further during stair ascent compared to walking (Appendix A-A). Therefore, each locomotion mode requires a specific algorithm to control the knee joint. [1]

Since there are multiple locomotion modes, transitions between these control algorithms are necessary. A sudden switch between these may lead to excessive mechanical work by the A-MPK. This can then disturb the balance of the user [2]. To prevent this, smooth transitions between locomotion modes are required. These transitions should not require cognition of the user and should happen reliably and safely [3]. To obtain smooth transitions, recognizing the user's intent is crucial [4].

Two aspects are important for the user's intent: the timing of the decision and the decision itself. When the user decides to switch locomotion mode, the control algorithm should be switched accordingly and at the right moment, to prevent user instability. This timing is referred to as the critical timing. Huang et al. [5] analyzed the critical timing for transitions between level-ground walking (LW) and stair ascent (SA). In this study, critical timing has been defined as the beginning of the swing phase for transitions to SA and the initial contact of the prosthetic foot for transitions to LW [5]. However, Simon et al. [6] have shown that a delay of 90 ms does not affect the stability of the user. Furthermore, delaying the transitions significantly increased the accuracy of the intent recognition algorithm [6].

As for the decision of the locomotion mode switch: it can be based on a combination of data from a variety of sensors. Besides the aforementioned IMU and load cell, additional equipment such as laser distance meters [7], [8], pressure sensors under the sole [9], electrical sensors on the sound leg [5] can be integrated. This additional equipment makes the device more complex and therefore more challenging to apply in daily use [5]. For example, electromyographic (EMG) signals are not stationary [5] and acquisition and implementation of lower limb prosthesis control during the dynamic task of ambulation is challenging [10]. Furthermore, the commercial market favors simplistic methods for intent recognition [11]. Thus, additional sensors are not desirable.

When analyzing sensor data, intent recognition can be implemented with two main approaches: a rule-based approach and a machine learning model [1]. Rule-based systems threshold parameters such as knee height to differentiate between locomotion modes. Several variations of rule-based systems for intent recognition have been proposed. For example, Grimes et al. [12] have developed a rule-based system to transition between LW and SA that was based on the knee angle at the contact of the foot with the floor. Parri et al. [13] have used a combination of ground reaction forces, joint angles of knee and hip, and angular velocities of the thighs, shanks, and feet. Jang et al. [14] have used the hip angle and absolute difference between the hip angles to recognize transitions from LW to SA. However, this algorithm resulted in a one-step delay of locomotion mode recognition, which is not desirable. Li et al. [15] have used a threshold on the vertical position of the IMU and the pitch angle of the foot. These thresholds were determined based on previously obtained data.

Rather than extracting and thresholding a specific combination of parameters, one can apply machine learning to utilize the entire data set. Machine learning models make predictions by building a mathematical model based on training data. For example, Huang et al. [5] and Zhang et al. [4] have combined EMG signals with mechanical signals in a support vector machine (SVM). Huang et al. [16] used EMG signals in a linear discriminant analysis (LDA) and an artificial neural network (ANN) classifier. The LDA's performance is comparable to the ANN, but the LDA was found to be more computationally efficient. For a more detailed overview, see appendices A-B and A-C. Out of various approaches for intent recognition with mechanical sensors and an IMU, previous work showed that the SVM was the most successful at predicting transitions between locomotion modes [17].

However, further investigation of data features is necessary to optimize the system for practical use [5]. As mentioned before, no consensus has been reached on the critical timing. Similarly, Huang et al. [5] and Zhang et al. [4] used sliding windows of 150 ms but did not report the reasoning for this choice. Later, Zhang et al. [2] analyzed the effect of timing to switch locomotion mode during transitions, but did not analyze transitions between LW and SA. Further research on the timing is crucial to improve the quality of intent recognition systems for A-MPKs. SVM has shown to be the most successful at predicting these transitions, and therefore should be best suited to elucidate the effects of the timing on intent recognition accuracy.

The objective of this study is to analyze the critical timing to switch locomotion modes and develop an SVM with mechanical sensor input for intent recognition. This SVM can differentiate between level-ground walking (LW), stair ascent (SA), and transitions between the two. Optimization of the SVM will be evaluated, along with the added value of subject-specific classifiers.

II. Methods

A. Materials

The A-MPK used in this study was the IntelLeg Knee (ILK), equipped with an IMU and a load cell (fig. 1). Furthermore, the ILK featured an embedded controller including control algorithms for LW and SA. Parameters that were logged during data acquisition were knee angles, knee velocity, knee acceleration, load cell axial force and sagittal bending moment.

The algorithm to control the knee used a global state machine with four different states: vertical tracking, powered extension, damped state, and swing state (fig. 2). Vertical tracking ensured a vertical shank orientation. The knee was extended during the powered extension state. The damped state supported the user during the stance phase. During swing state, the knee flexed to provide ground clearance and subsequently extended for foot placement.

The embedded control algorithms for LW and SA used different combinations of states available in the global state machine. The control algorithm for LW switched back and forth between swing state and damped state. SA's control algorithm was slightly more extensive: once the foot was in the swing state, the ILK would go to the vertical tracking state. Once the foot was placed on the stairs, the ILK would go to the damped state, after which the powered extension state supported the user during step-over-step stair ascent. Within the swing state, there were sub-states, which defined the control algorithm for a specific locomotion mode. For example, the minimum knee angle was around -60 degrees during LW and -90 degrees during SA (θ_{knee} in fig. 1b).

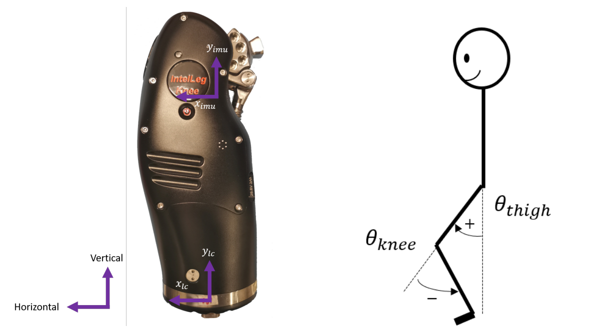

(a) Side view of the ILK and the definitions of axes

(b) Definition of knee and thigh angle. Thigh angles were estimated based on the IMU and the Madgwick algorithm

Fig. 1: ILK and the used definitions

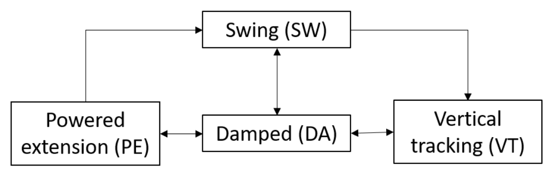

Fig. 2: Global state machine and transitions between the states.

As noted before, the ILK contained an embedded controller. Besides supporting SA and LW, the controller featured a rule-based switch to switch between these modes. The decision to switch control algorithms was based on the vertical position of the IMU. More specifically, the switch from LW to SA was made when the IMU's vertical position rose more than 7.5 cm.

Besides the ILK, further materials used to gather data are an L-shaped socket, a body-weight support system, and a wired connection with a laptop. The L-shaped socket was used in combination with the ILK, to allow able-bodied subjects to walk with the ILK. The body-weight support system (ZeroG, Aretech LLC) was used for safety, of which the track had a rectangular shape (fig. 3). The wired connection allowed communication between Simulink and the ILK, to manually trigger transitions between control algorithms. The sampling frequency was 1000 Hz.

B. Participants and database generation

TABLE I: Summary of demographic information for the three able-bodied subjects (H1-H3)

	Length (m)	Weight (kg)	Age	Gender
H1	1.83	85	32	M
H2	1.62	72	28	F
H3	1.71	67	25	F

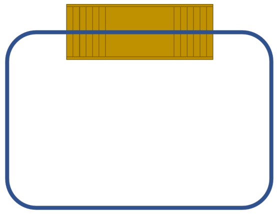

Fig. 3: Upper view of the track. The blue line represented the rail of the body-weight support system, the brown object represented the stairs with a horizontal part in the middle

Three able-bodied subjects (see table I for demographic information), all familiar with using the ILK, were included in the study. To gather training data, subjects performed 20 laps: 10 times clockwise, 10 times counter-clock-wise. To avoid fatigue, subjects were allowed to rest, on request. Each lap consisted of LW, a transition from LW to SA, steady-state SA, transition from SA to LW, descending the stairs, and level-ground walking until the starting point (fig. 3). Through Simulink, the conductor of the experiment initiated the switch between locomotion modes, which took place at toe-off. So, for a transition from LW to SA, the control algorithm of LW would be used, until the prosthetic foot left the floor. Toe-off was detected if the bending rate of change was larger than 1 Nm/kgs and the axial load was smaller than -1% of the body weight of the user.

Based on the IMU and load cell data, other variables were calculated: yaw angle, pitch angle, roll angle, stride height, stride length, stride velocity in the horizontal and vertical direction.

C. Critical timing

The knee angle followed roughly the same pattern for LW and for the transition between LW and SA, up to a certain point in the gait cycle. The same holds for transitions from SA to LW. A smooth transition occurred when the switch was made before the difference between the control algorithms became too large. To be more specific, in this study the threshold for this difference was defined as an absolute difference of 10 degrees. The moment in time after toe-off that the difference exceeds the threshold is defined as the critical timing.

D. Training the SVM classifier

The machine learning approach consisted of multiple parts (fig. 4). The developed classifier was trained to decide before the critical timing.

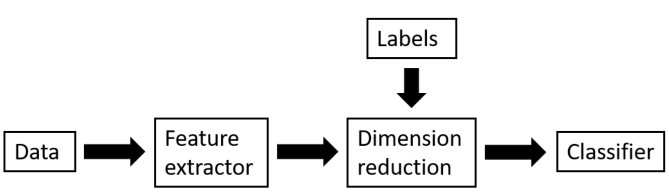

Fig. 4: Flowchart for training the classifier

1) Labels: steady-state LW, a transition from LW to SA, steady-state SA, or a transition from SA to LW. Labeling was done manually, by analyzing the combination of maximum thigh flexion angles and minimum knee flexion angles for each step and comparing them to those of the previous step.

2) Feature extraction: as noted before, data was gathered at 1000 Hz. Furthermore, data during the complete gait cycles was logged. However, only the data before the critical timing was of interest for the intent recognition system. Therefore, for every gait cycle, specific features were extracted from this portion of the data. These features consisted of the minimum, maximum, and mean value, and the standard deviation for each logged and derived parameter from the IMU and load cell.

3) Dimension reduction: To reduce complexity of the system, dimension reduction was used. LDA was used to transform the data set, consisting of all the parameters, into a lower-dimensional data set. LDA transformed the data, such that the distances between classes were maximized (Appendix A-C1). This resulted in an n by m matrix, with n the number of analyzed gait cycles and m the number of classes minus one.

4) SVM Classifier: hyperparameter optimization of the SVM was done by the automatic optimization algorithm of MATLAB, which uses Bayesian optimization.

E. Manual optimization of the SVM

Besides optimization of the SVM within MATLAB, changes can be made to the input data as well. In this case, the effect of the following aspects were analyzed: the number of subjects, the window size and delay, and the use of sub-classes.

1) Number of subjects: data was gathered from three subjects. By comparing the performance of the SVM trained on all the subjects with the SVM trained on a specific subject, the added value of subject-specific SVMs can be assessed.

2) Window size and delay: the effect of using various portions of the data on the accuracy of the SVM was assessed as well. First, from toe-off, a variable delay was introduced. This delay ranged from -500 to 100 ms, in increments of 100 ms. From this point in time, data was selected within a window of variable size. The used window sizes were 100, 200, 300, or 400 ms. Based on the combination of the delay and window size, a specific portion of the data was analyzed. The accuracy of the optimized model was estimated for all the combinations of delays and window sizes.

3) Number of classes: to assess the effect of the number of classes on the accuracy of the SVM, two types of models were used. The 4-class model consisted of steady-state LW and SA, and the transitions between the two. For the 2-class model, the steady-state data and the transitional data were merged into one class. For example, data from steady-state LW and the transition from SA to LW were merged into one class.

F. System evaluation

Various analyses were performed. First, a general analysis of walking gait was done on the individual subjects. Then, the critical timing was evaluated for each subject and compared to the timing of the embedded rule-based intent recognition system.

The effects of the aforementioned factors (section II-E) on the accuracy of the SVM were analyzed. Lastly, the generalization of the models was evaluated. These effects were tested with the following indicators of classification accuracy:

$$\text{Accuracy} = \frac{\text{\# of correct classified observations}}{\text{total \# of observations}} \quad (1)$$

$$\text{fSA} = \frac{\text{\# of falsely classified SA}}{\text{total \# of classified SA}} \quad (2)$$

$$\text{fLW} = \frac{\text{\# of falsely classified LW}}{\text{total \# of classified LW}} \quad (3)$$

10-fold cross-validation was applied to obtain the confusion matrix. The indicators were deduced from this confusion matrix.

This resulted in a confusion matrix, from which the indicators were deduced. The accuracy gave a general idea of the performance of the SVM, which should be maximized. Whereas the false SA rate (fSA) and the false LW rate (fLW) indicated the origin of misclassification, which should be minimized. However, minimization of fSA should be prioritized, since false SA classification was likely to result in the user falling down. False LW classification was likely to result in inability to ascend the stairs in a step-over-step manner. This is inconvenient and uncomfortable for the user, but not necessarily dangerous.

To analyze the generalizability of the subject-specific models, the data of the other subjects were used as input. The same accuracy indicators were then calculated.

III. Results

A. Analysis of locomotion modes

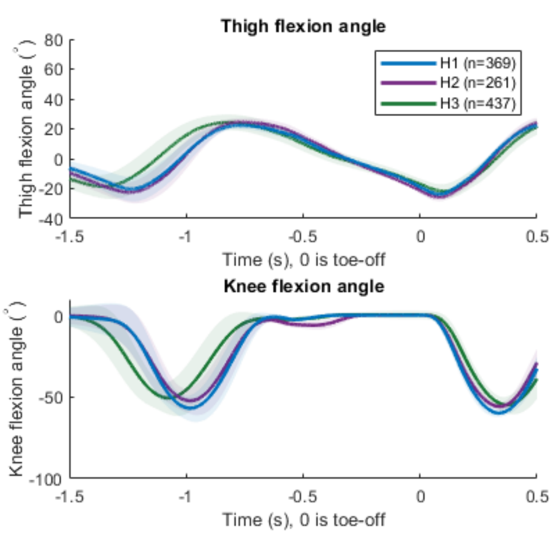

Fig. 5: Mean ± SD knee and thigh flexion angles of steady-state LW. t=0 represents the toe-off event of the current step. Maximum knee flexion reaches a knee angle of -60 degrees. n was the number of steps that were analyzed per subject

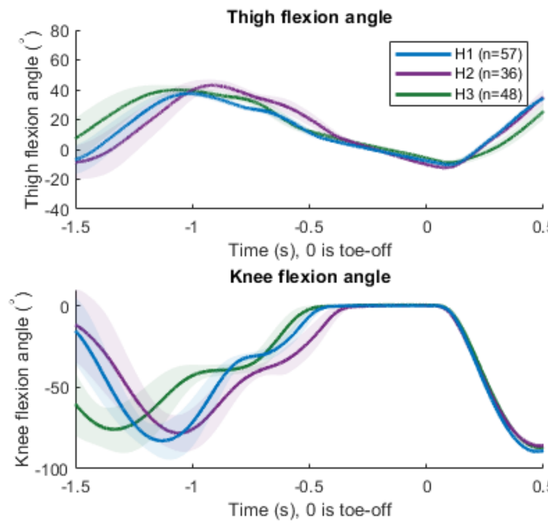

Fig. 6: Mean ± SD knee and thigh flexion angles of steady-state SA. t=0 represents the toe-off event of the current step. Maximum knee flexion reaches a knee angle of -90 degrees. n was the number of steps that were analyzed per subject

Each subject had a slightly different locomotion pattern (see fig. 5 and fig. 6). The reached angles were comparable, but the timing of the peaks varied. This might have consequences for the critical timing and optimal window per subject. During steady-state LW, H3 had a longer stance phase than the other two subjects. Furthermore, H2 had a slight knee flexion during the stance phase, while the other two subjects kept a knee angle of approximately 0 degrees. During the steady-state SA, H3 needed more time to extend the knee. H2 had a slightly larger thigh flexion and slightly smaller knee angle.

B. Critical timing

Transitions from SA should be made before 340 ms after toe-off (fig. 7). The rule-based controller would have taken this decision at 180 ms after toe-off. However, it can be seen that the critical timing varied among subjects: between 340 and 370 ms after toe-off.

For transitions from LW, the decision should be taken a little bit earlier: 230 ms after toe-off. The rule-based controller would have decided 260 ms after toe-off (fig. 8). The critical timing with the manual switch varies a bit more among the subjects: between 220 ms and 300 ms after toe-off.

The smallest value of the critical timing was 220 ms after toe-off. Therefore, the used windows ended at 200 ms after toe-off.

C. Manual optimization of the SVM

1) Optimization per subject: The performance of the subjects depended on the choice of window size and delay (fig. 9). The locations and values of the maxima of the accuracy varied among the subjects and used number of classes. The maximum accuracy was for the 4-class model of H3: 99.81%. This model uses a window of 0:100.

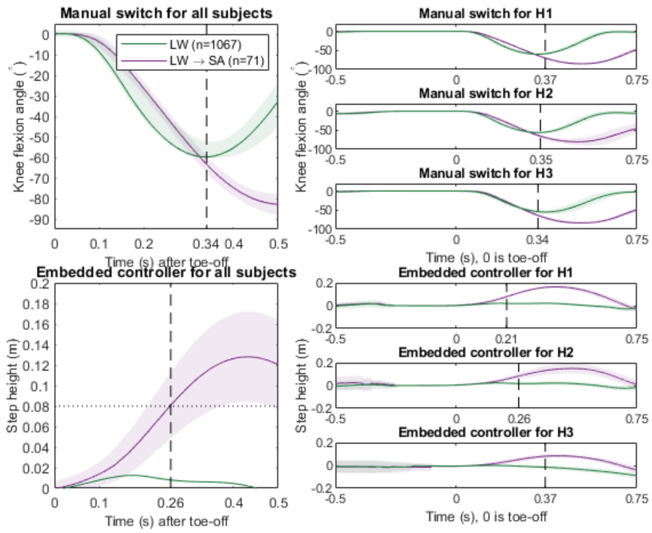

Fig. 7: Critical timing for transitions from LW. The critical timing varied for each subject. t=0 represents the toe-off event of the current step. The upper half shows the results for the manual transitions, the lower half shows the results for the embedded rule-based controller. The left half shows the averaged results, while the right half shows the results per subject.

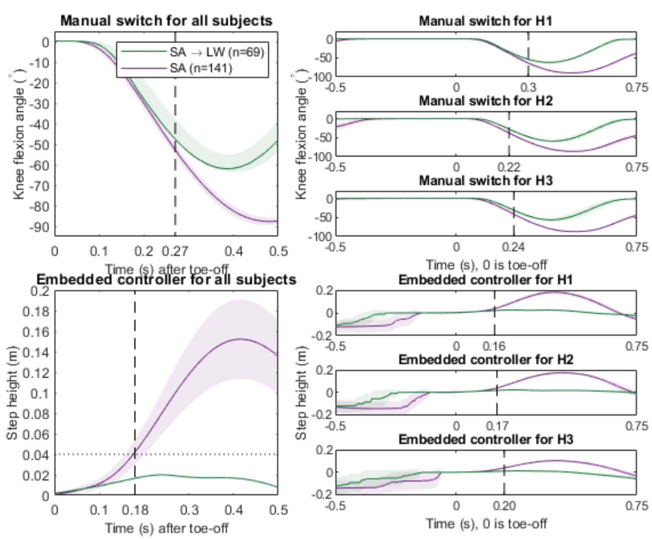

Fig. 8: Critical timing for transitions from SA. The critical timing varies for each subject. t=0 represents the toe-off event of the current step. The upper half shows the results for the manual transitions, the lower half shows the results for the embedded rule-based controller. The left half shows the averaged results, while the right half shows the results per subject.

a) H1: The 4-class and 2-class models all resulted in the same value for accuracy: 99.79%. Furthermore, the values for fSA and fLW were equal, 0% and 0.25% respectively. There was one exception: for a window of -200:200, fSA was 1.20% and fLW was 0%. Remarkably, the locations of the maxima were equal for the 4-class and 2-class models.

b) H2: The 4-class model resulted in one model with an accuracy of 99.40%. fSA was 1.85% and fLW was 0.36%. The window for which this held was -100:200. The 2-class model resulted in 10 possible models with an accuracy of 99.09%. Four of those had the lowest possible fSA: 1.89% and a fLW of 0.72%. The windows for which this held are -500:-300, -400:-300, 0:200 and 100:200.

c) H3: The 4-class model resulted in one model with an accuracy of 99.81%, fSA of 1.30%, and fLW of 0% for the window -500:-100. For the 2-class models, 8 models resulted in an accuracy of 99.63%, fSA of 2.56% and fLW of 0%. The windows for which this held are -300:100, -200:100, -200:200, -100:100, -100:200, 0:100, 0:200, and 100:200.

2) General model: The accuracy of the combined model varied for the combination of window size, delay, and the number of classes. The maximum accuracy for the 4-class model was 99.41%, there was one model with this accuracy for a window of -200:200. fSA was 2.78% and fLW was 0.18%. For the 2-class model, the maximum accuracy was 99.33%. There were 6 models with this accuracy, and they all had a fSA of 2.79% and fLW of 0.26%. The windows were -200:100, -200:200, -100:200, 0:100, 0:200, and 100:200.

The feature space (fig. 11) of the combined 4-class model shows that there was variability among the subjects. The cloud for the classes was more spread out and sometimes data points cross clouds. For example, this can be seen fig. 11b, where multiple data points from LW $\rightarrow$ SA of H2 and H3 were closer to the cloud with SA $\rightarrow$ LW than of their class.

3) Number of classes: The distances between the separate classes in the feature space for the 4-class model were visible (fig. 12), while these distances were less clear in the feature space for the 2-class model. This could also be seen in the accuracy of the models: the 4-class models were slightly more accurate than the 2-class models (table II). The largest difference was for H3: fSA was 1.30% for the 4-class model, compared to 2.56% for the 2-class model. However, it should be noted that these models used a separate delay and window size (fig. 9). On the other hand, the number of possible models for the combined data set with 2 classes was larger than for the 4 classes, with slightly lower accuracy.

D. Generalization of the models

The optimum window changed strongly when the data of the other subjects was used as input for the subject-specific models (fig. 14). The overall accuracy of all the models dropped: the highest accuracy of all models was 91.74% (table III), compared to 99.81% for the subject-specific model. Furthermore, fSA was a lot higher. The feature spaces of the different subjects are shown in fig. 13. It can be seen that the shape of the feature spaces was comparable, but the values had a different offset.

IV. Discussion

A. Interpretation of results

1) Critical timing: The critical timing of the transition from SA was found to be 270 ms after toe-off but varied among the subjects. The rule-based controller was slightly faster with

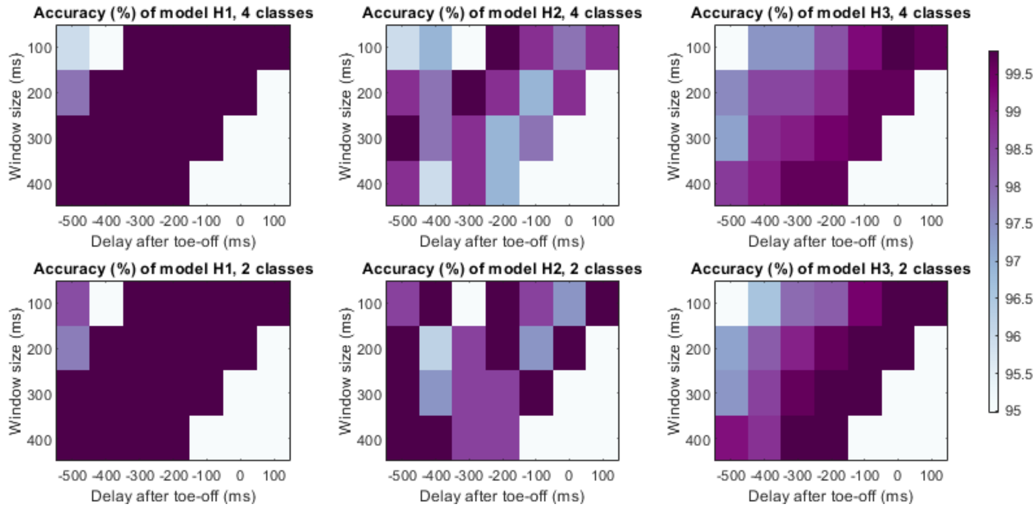

Fig. 9: Accuracy of each cross-validated model for all subjects and combinations of window sizes, delays, and number of classes

TABLE II: Overview of accuracy of 4-class models and 2-class models

	4-class model				2-class model			
	# of models	**Accuracy (%)**	**fSA (%)**	**fLW (%)**	**# of models**	**Accuracy (%)**	**fSA (%)**	**fLW (%)**
H1	19	99.79	0	0.25	18	99.79	0	0.25
H2	1	99.40	1.85	0.36	4	99.09	1.89	0.72
H3	1	99.81	1.30	0	8	99.63	2.56	0
Combined	1	99.41	2.78	0.18	6	99.33	2.79	0.26

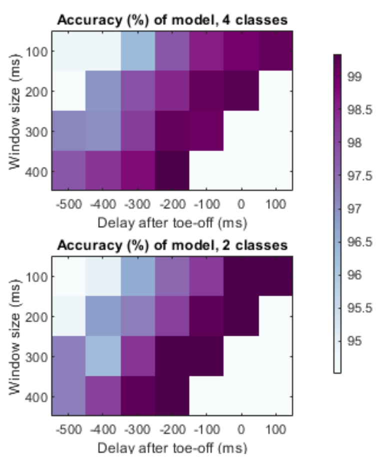

Fig. 10: Accuracy of the cross-validated combined model for all combinations of window sizes, delays, and number of classes

a decision time of 230 ms after toe-off. The transition from LW was 340 ms after toe-off, the rule-based controller was faster with 250 ms after toe-off. This suggests that there is more time to decide than the rule-based system uses.

Furthermore, there was some variability among subjects. This suggests that the differences in locomotion patterns also result in a unique value for the critical timing. This affects the to be studied windows and delays: if a decision has to be made earlier in the gait cycle, there is no use in analyzing the data.

TABLE III: Summary of results of generalization of the models

Model	**Accuracy (%)**	**False SA (%)**	**False LW (%)**	**Window (ms after toe-off)**
H1, 4 classes	71.05	92.68	4.92	0:100
H1, 2 classes	85.71	2	14.38	-500:-300
H2, 4 classes	75.02	27.50	0	-500:-400
H2, 2 classes	83.78	51.78	7.68	-500:-400
H3, 4 classes	89.89	7.41	1.26	-500:-400
H3, 2 classes	91.74	16.50	7.06	-500:-400

Zhang et al. [2] seem to be the only ones that have tried to quantify the critical timing of transitions as well, based on the mechanical work that has been done by the A-MPK. However, since that has not been analyzed in this study, it is not possible to compare the criterion with the value used in this study.

2) Optimization of the classifier:

a) Subject-specific vs general model: The performance of the classifier has been analyzed for a data set consisting of one and a data set consisting of three subjects. For both the 4-class model and the 2-class model, the accuracy was lower for the combined model than for the individual subjects. This suggests that subject-specific models outperform general models. This is in agreement with Young et al. [18]

b) Number of classes: Combining the transitional data and steady-state data in one class resulted in a slightly less accurate model. However, the differences between the accuracy were less than 0.4%. The value of fSA was slightly higher for the 2-class model. Furthermore, more models could result in the same accuracy.

Young et al. [18] also analyzed the number of classes, but

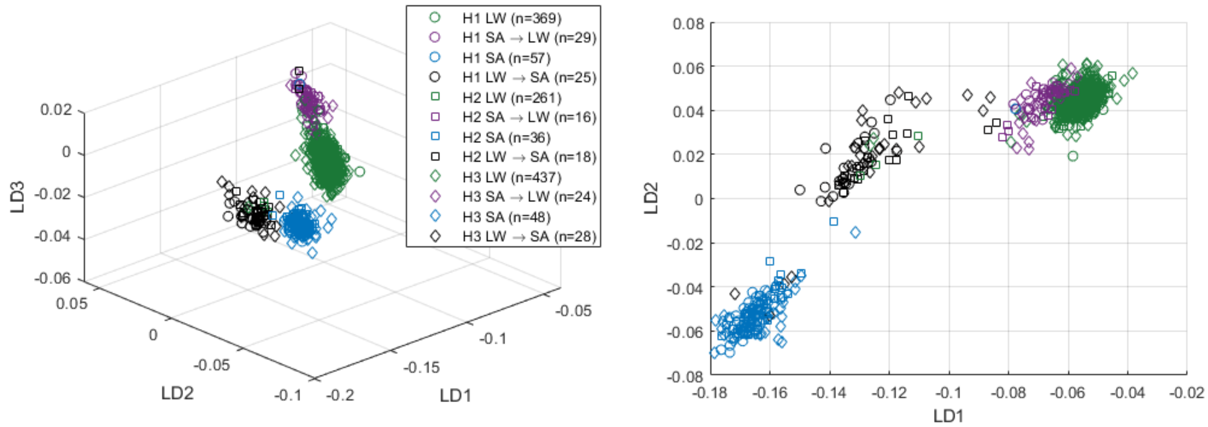

(a) Feature space of the combined model in 3D

(b) Feature space of the combined model in 2D

Fig. 11: Feature space of the combined model for the window -200:200 ms after toe-off

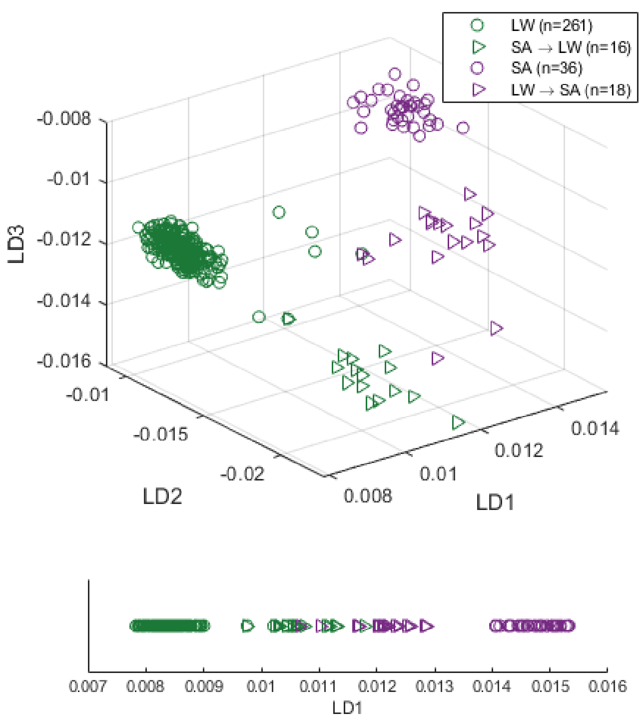

Fig. 12: Comparison of the feature space for the 4-class model (top) and 2-class model (bottom) and window -100:200

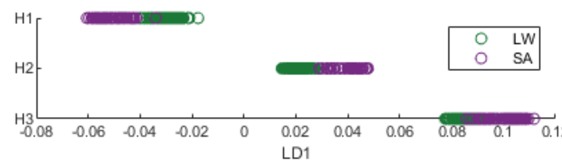

Fig. 13: Feature space for the model of H1 with 2 classes and window -500:-300

took a different approach. They built a 5-class model in which transitional and steady-state data were merged into one class, and they built a mode-specific model in which the steady-state and transitional data were split into two classes. This resulted in more accurate predictions for the mode-specific model. However, no conclusion is drawn on whether or not merging steady-state and transitional data into one class is beneficial.

c) Window size and delay: The various data sets resulted in diverse combinations of window size and delays. The models of H1 with 4 classes resulted in a lot of combinations that all accurately predicted the locomotion mode. For the other subjects and the 4-class models, only one model resulted in the best accuracy. For the 2-class models, a minimum of 4 and a maximum of 18 models resulted in the best accuracy. The window size and delay depended on the subject-specific data set, which suggests that they depend on the gait pattern of the user. Zhang et al. [4] used a sliding window of 150 ms. Huang et al. [5] report predictions of the classifiers approximately 300-420 ms before the prosthetic foot left the ground. In this study, it is possible to predict the intention of the next step up to 400 ms before toe-off. Furthermore, this study has shown that it is possible to do so after toe-off. However, this is at the cost of accuracy.

d) Features used in classifier: The features used in this study where the minimum, maximum, mean, and standard deviation of the parameter for that specific window. Zhang et al. [4] use the mean, standard deviation, minimum, and maximum values of each parameter for the mechanical signals. The used mechanical signals were the forces and moments recorded by a 6-DOF load cell mounted on the prosthetic pylon. Huang et al. [5] also use the minimum, maximum, and mean value of each direction of force or moment. This study shows that the prediction of locomotion mode can be done by less complex system as well, which fits perfectly to the conclusion of Fluit et al. [11]: simplistic methods with mechanical sensors for intent recognition are favored by the commercial market, which is the end goal for this product.

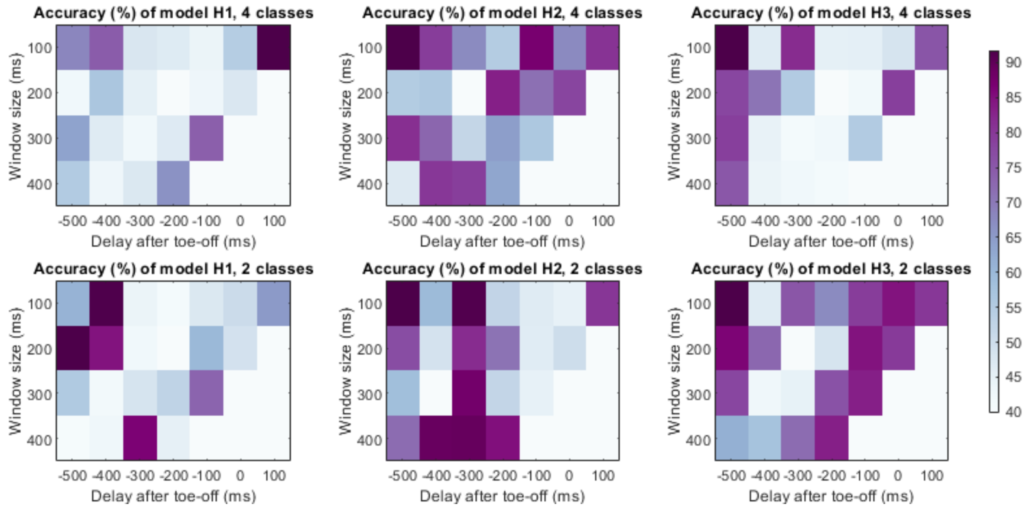

Fig. 14: Accuracy of the model predicting the locomotion mode of the other subjects

e) Offline performance of machine learning approach: For the data set with one subject, the classifier was able to successfully predict the locomotion mode with an accuracy of 99.81%. Huang et al. [5] reached an accuracy of 95% for recognizing the transitional periods. Li et al. [15] obtained an accuracy of at least 92%. This study resulted in higher accuracy values for all models that were considered.

3) Generalization of model: It was shown that the accuracy of the models drastically decreases if data of other subjects are used for the subject-specific models. This supports the earlier observation that a subject-specific model results in more accurate results.

B. Limitations and recommendations

The amount of data that has been gathered was limited: only three subjects have been included, with 15 samples of the locomotion mode transitions. Variables such as walking speed, different angles of approaching the stairs, or different types of stairs, have not been taken into account. Therefore, the models developed in this study might lack robustness in real-life situations. Using a larger number of samples in various environments should increase the robustness of the system. On the other hand, there is a trade-off between the burden on the user to obtain a large data set and the improvement of accuracy and robustness. In future research, this trade-off should be investigated.

As mentioned in the methods for participant and database generation (section II-B), the conductor of the experiment initiated the switch between locomotion modes. The switch of control algorithms then took place at toe-off. As a result, the subjects might move differently compared to when only the LW control was used. This may have affected the acquired data and therefore might have consequences for real-time implementation. To solve this, data should be gathered where the switch between locomotion modes takes place at the critical timing rather than toe-off.

The threshold used to estimate the critical timing was 10 degrees. It was assumed that a threshold this strict would result in smooth locomotion mode transitions. However, these assumptions should be tested in real-time. Zhang et al. [19] analyzed the mechanical work done by the prosthesis to predict whether or not this transition would cause instability of the user. This measure can be used to assess this assumption.

It was shown that a subject-specific model resulted in a more accurate prediction than the general model. It might be interesting to look at the possibilities of generating a general model, which can be adapted to the user, to make it user-specific. This can be done by for example reinforcement learning or by expanding the training data set for the specific user. This would reduce the burden on the user during initial training.

The benefit of a machine learning approach over a rule-based approach for intent recognition systems has not been shown yet. Along with real-time implementation, it would be interesting to analyze the differences and user preference between the two approaches.

Lastly, to be able to bring this product to the market, several steps have to be taken. First of all, rather than doing offline analysis, the intent recognition algorithm should be executed solely on the ILK and in real-time. Furthermore, support for additional locomotion modes, such as ramp ascent, should be implemented as well. However, this will make the intent recognition system more complex, and will therefore need more research.

V. Conclusion

An SVM to predict locomotion mode transitions between LW and SA was developed. To do so, data of these transitions has been gathered by manually switching between locomotion modes at toe-off. To safely transition between the different locomotion modes, the decision of the SVM must be made before the critical timing of 220 ms after toe-off. This value was subject-dependent and ranged between 220 ms and 300 ms.

Offline optimization of the SVM shows that estimating the critical timing is feasible. Furthermore, characteristics of the SVM input data, such as window size and delay, were subject-specific. A subject-specific SVM resulted in the highest accuracy values. Finally, there was no large difference between merging the transitional and steady-state data into one class, compared to separating them into individual classes.

REFERENCES

[1] M. R. Tucker, J. Olivier, A. Pagel, H. Bleuler, M. Bouri, O. Lambercy, J. del R Millán, R. Riener, H. Vallery, and R. Gassert, "Control strategies for active lower extremity prosthetics and orthotics: a review," *Journal of neuroengineering and rehabilitation*, vol. 12, no. 1, p. 1, 2015.

[2] F. Zhang, M. Liu, and H. Huang, "Investigation of timing to switch control mode in powered knee prostheses during task transitions," *PLOS one*, vol. 10, no. 7, p. e0133965, 2015.

[3] H. A. Varol, F. Sup, and M. Goldfarb, "Multiclass real-time intent recognition of a powered lower limb prosthesis," *IEEE Transactions on Biomedical Engineering*, vol. 57, no. 3, pp. 542–551, 2010.

[4] F. Zhang, Z. Dou, M. Nunnery, and H. Huang, "Real-time implementation of an intent recognition system for artificial legs," in *Conference proceedings:... Annual International Conference of the IEEE Engineering in Medicine and Biology Society. IEEE Engineering in Medicine and Biology Society. Conference*, vol. 2011. NIH Public Access, 2011, p. 2997.

[5] H. Huang, F. Zhang, L. J. Hargrove, Z. Dou, D. R. Rogers, and K. B. Englehart, "Continuous locomotion-mode identification for prosthetic legs based on neuromuscular–mechanical fusion," *IEEE Transactions on Biomedical Engineering*, vol. 58, no. 10, pp. 2867–2875, 2011.

[6] A. M. Simon, K. A. Ingraham, J. A. Spanias, A. J. Young, S. B. Finucane, E. G. Halsne, and L. J. Hargrove, "Delaying ambulation mode transition decisions improves accuracy of a flexible control system for powered knee-ankle prosthesis," *IEEE Transactions on Neural Systems and Rehabilitation Engineering*, vol. 25, no. 8, pp. 1164–1171, 2016.

[7] L. Du, F. Zhang, M. Liu, and H. Huang, "Toward design of an environment-aware adaptive locomotion-mode-recognition system," *IEEE Transactions on Biomedical Engineering*, vol. 59, no. 10, pp. 2716–2725, 2012.

[8] M. Liu, D. Wang, and H. H. Huang, "Development of an environment-aware locomotion mode recognition system for powered lower limb prostheses," *IEEE Transactions on Neural Systems and Rehabilitation Engineering*, vol. 24, no. 4, pp. 434–443, 2016.

[9] Z. Liu, W. Lin, Y. Geng, and P. Yang, "Intent pattern recognition of lower-limb motion based on mechanical sensors," *IEEE/CAA Journal of Automatica Sinica*, vol. 4, no. 4, pp. 651–660, 2017.

[10] J. Spanias, A. Simon, S. Finucane, E. Perreault, and L. Hargrove, "Online adaptive neural control of a robotic lower limb prosthesis," *Journal of neural engineering*, vol. 15, no. 1, p. 016015, 2018.

[11] R. Fluit, E. Prinsen, S. Wang, and H. Van Der Kooij, "A comparison of control strategies in commercial and research knee prostheses," *IEEE Transactions on Biomedical Engineering*, 2019.

[12] D. L. Grimes, "An active multi-mode above knee prosthesis controller," Ph.D. dissertation, Massachusetts Institute of Technology, 1979.

[13] A. Parri, E. Martini, J. Geeroms, L. Flynn, G. Pasquini, S. Crea, R. Molino Lova, D. Lefeber, R. Kamnik, M. Munih *et al.*, "Whole body awareness for controlling a robotic transfemoral prosthesis," *Frontiers in neurorobotics*, vol. 11, p. 25, 2017.

[14] J. Jang, K. Kim, J. Lee, B. Lim, and Y. Shim, "Online gait task recognition algorithm for hip exoskeleton," in *2015 IEEE/RSJ International Conference on Intelligent Robots and Systems (IROS)*. IEEE, 2015, pp. 5327–5332.

[15] Y. D. Li and E. T. Hsiao-Wecksler, "Gait mode recognition and control for a portable-powered ankle-foot orthosis," in *2013 IEEE 13th International Conference on Rehabilitation Robotics (ICORR)*. IEEE, 2013, pp. 1–8.

[16] H. Huang, T. A. Kuiken, R. D. Lipschutz *et al.*, "A strategy for identifying locomotion modes using surface electromyography," *IEEE Transactions on Biomedical Engineering*, vol. 56, no. 1, pp. 65–73, 2009.

[17] M. Penubaku, "Locomotion intent recognition using a multimodal sensor fusion approach," Master's thesis, TU Delft, 9 2018, confidential until 07-09-2023.

[18] A. J. Young and L. J. Hargrove, "A classification method for user-independent intent recognition for transfemoral amputees using powered lower limb prostheses," *IEEE Transactions on Neural Systems and Rehabilitation Engineering*, vol. 24, no. 2, pp. 217–225, 2016.

[19] F. Zhang, M. Liu, and H. Huang, "Effects of locomotion mode recognition errors on volitional control of powered above-knee prostheses," *IEEE Transactions on Neural Systems and Rehabilitation Engineering*, vol. 23, no. 1, pp. 64–72, 2014.

[20] C. Vaughan, B. Davis, and J. O'Connor, *Dynamics of Human Gait*, 2nd ed. Kiboho Publishers, 1992.

[21] S. M. Reid, S. K. Lynn, R. P. Musselman, and P. A. Costigan, "Knee biomechanics of alternate stair ambulation patterns," *Medicine & Science in Sports & Exercise*, vol. 39, no. 11, pp. 2005–2011, 2007.

[22] A. Novak, S. Reid, P. Costigan, and B. Brouwer, "Stair negotiation alters stability in older adults," https://lermagazine.com/article/stair-negotiation-alters-stability-in-older-adults, 10 2010.

[23] J. Brownlee, *Master Machine Learning Algorithms: discover how they work and implement them from scratch*. Jason Brownlee, 2016.

[24] S. Raschka, "Linear discriminant analysis - bit by bit," https://sebastianraschka.com/Articles/2014_python_lda.html#summarizing-the-lda-approach-in-5-steps, 8 2014, visited on 03-12-2019.

[25] X. Wang and K. K. Paliwal, "Feature extraction and dimensionality reduction algorithms and their applications in vowel recognition," *Pattern recognition*, vol. 36, no. 10, pp. 2429–2439, 2003.

[26] A. Meyer-Baese and V. Schmid, "Chapter 2 - feature selection and extraction," in *Pattern Recognition and Signal Analysis in Medical Imaging (Second Edition)*, second edition ed., A. Meyer-Baese and V. Schmid, Eds. Oxford: Academic Press, 2014, pp. 21 – 69. [Online]. Available: http://www.sciencedirect.com/science/article/pii/B9780124095458000029

[27] I. K. center, "Total variance explained," https://www.ibm.com/support/knowledgecenter/en/SSLVMB_24.0.0/spss/tutorials/fac_cars_tve.html, visited on 02-03-2020.

[28] K. Fite, J. Mitchell, F. Sup, and M. Goldfarb, "Design and control of an electrically powered knee prosthesis," in *2007 IEEE 10th International conference on rehabilitation robotics*. IEEE, 2007, pp. 902–905.

[29] F. Sup, A. Bohara, and M. Goldfarb, "Design and control of a powered knee and ankle prosthesis," in *Proceedings 2007 IEEE International Conference on Robotics and Automation*. IEEE, 2007, pp. 4134–4139.

[30] A. J. Young, A. M. Simon, and L. J. Hargrove, "A training method for locomotion mode prediction using powered lower limb prostheses," *IEEE Transactions on Neural Systems and Rehabilitation Engineering*, vol. 22, no. 3, pp. 671–677, 2014.

[31] R. B. Woodward, J. A. Spanias, and L. J. Hargrove, "User intent prediction with a scaled conjugate gradient trained artificial neural network for lower limb amputees using a powered prosthesis," in *Engineering in Medicine and Biology Society (EMBC), 2016 IEEE 38th Annual International Conference of the*. IEEE, 2016, pp. 6405–6408.

[32] H. A. Varol, F. Sup, and M. Goldfarb, "Real-time gait mode intent recognition of a powered knee and ankle prosthesis for standing and walking," in *2008 2nd IEEE RAS & EMBS International Conference on Biomedical Robotics and Biomechatronics*. IEEE, 2008, pp. 66–72.

[33] B. E. Lawson, J. Mitchell, D. Truex, A. Shultz, E. Ledoux, and M. Goldfarb, "A robotic leg prosthesis: Design, control, and implementation," *IEEE Robotics & Automation Magazine*, vol. 21, no. 4, pp. 70–81, 2014.

APPENDIX A
LITERATURE STUDY

This literature study gives background information concerning locomotion mode analysis and the differences between level-ground walking and stair ascent. Furthermore, different intention detection algorithms will be explained. Lastly, the used machine learning algorithms will be elaborated.

A. Locomotion mode analysis

To find the differences between the different locomotion modes and the best transition phases, it is important to understand the phases of the different locomotion modes. Level-ground walking and stair ascent are included.

1) Level-ground Walking (LW): Human gait is a periodic movement. There are two main phases in the gait cycle: stance and swing phase. During the stance phase, the foot is on the ground, while in the swing phase this foot is no longer in contact with the ground and the leg is swinging, in preparation for the next foot strike.
The stance phase can be subdivided into three phases [20]:

- First double support: Both feet are in contact with the ground
- Single limb stance: One foot is swinging through, the other is in contact with the ground
- Second double support: Both feet are in contact with the ground again

The gait cycle has been further subdivided into eight events, of which five are during the stance phase and three during the swing phase. These events are based on the movement of the foot. [20] Fig. 15 shows the visualization of the different gait events.

- Heel strike/contact: Initiates gait cycle. Represents the point at which the body's center of gravity is at the lowest position
- Foot-flat: The time when the sole touches the ground
- Mid-stance: When the swinging foot passes the stance foot and the body's center of mass is at the highest position.
- Heel-off: The heel loses contact with the ground and push-off is initiated by the calf muscles, which results in pointing the foot downwards.
- Toe-off: Termination of stance phase as the foot leaves the ground
- Acceleration: Starts as soon as the foot leaves the ground and the subject activates the hip flexor muscles to accelerate the leg forward
- Mid-swing: When the foot passes directly beneath the body, coincidental with mid-stance for the other foot
- Deceleration: Action of the muscle as they slow down the leg and stabilize the foot in preparation for the next heel strike.

However, it should be noted that this is the gait cycle for healthy humans. Research has shown that unilateral lower-limb amputees adapt their gait. They have a slower comfortable forward velocity, wider strides, and a shorter cycle. Furthermore, they show an asymmetric walking pattern. The prosthetic stance phase is shorter and the prosthetic swing phase is longer. The unaffected side shows the opposite: a longer stance phase and a shorter swing phase. The maximum flexion of the unaffected knee is larger than the prosthetic knee and the prosthetic step length is shorter. The prosthetic knee is locked in extension during most of the stance phase. Amputees show mediolateral displacement to keep the center of mass over the prosthesis during prosthetic single support. Lastly, the metabolic cost of walking is increased by 20 to 100%. [12], [5]

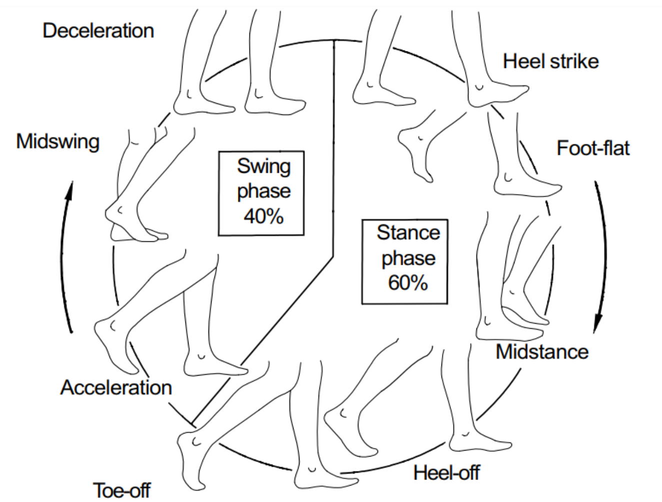

Fig. 15: Visualization of gait events. [20]

2) Stair ascent: There are different patterns to ascend stairs. Healthy individuals use a step-over-step (SOS) gait pattern. However, disabled populations may be forced to adjust their gait pattern because of decrements in muscular strength, altered balance mechanisms, etc. These populations often adopt alternate gait patterns, such as increased handrail use, sideways motion, or a step-by-step gait (SBS) gait pattern. For the SBS pattern, subjects place both feet on the same step before ascending or descending. The leading leg takes the step, the trailing leg is then lifted onto the same step. [21]

For the SOS gait pattern, there is a cyclic pattern while ascending stairs, visualized in Fig. 16. This cycle is divided into two distinct phases: the stance phase and the swing phase. During the ascent, the stance phase consists of three sub-phases: weight acceptance, pull-up, and forward continuance. During weight acceptance, the body is shifted such that the body is in an optimal position to be pulled up. During pull-up, the other leg is lifted and positioned on the next step for forward continuance. The swing phase is divided into two sub-phases: foot clearance and foot placement. During foot clearance the leg is raised, during foot placement, the swing leg is positioned for foot placement on the next step. [22]

B. Intention detection (ID)

Different methods are available for intention detection, such as echo control, rule-based detection, or machine learning

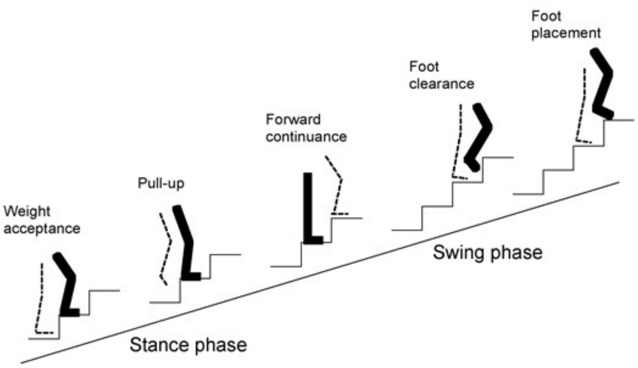

Fig. 16: Visualization of phases of stair ascent. (Edited from [22])

algorithms. All systems need input signals, such as input from the user, the prosthesis, or both. Signals originated from the body can be measured with an electromyography. The input signals coming from the prosthesis depend on the type of mechanical sensors that are available on the prosthesis. Examples of this are load cells and IMU.

The combination of EMG and mechanical sensor information outperformed the machine learning classifiers with only EMG or mechanical sensor information. [5] However, using EMG signals also results in a complex system: EMG signals are not stationary [5], acquisition, and implementation of lower limb prosthesis control during the dynamic task of ambulation is challenging. This may result in a questionable quality of EMG data. [10] Results of Huang et al. [16] suggest that sufficient neural control information can be extracted for accurate classification of locomotion mode from EMG signals recorded from muscle above the knee in able-bodied subjects and possibly individuals with long trans-femoral (TF) amputations. Therefore, it is unclear whether this is feasible in subjects with short amputations. Spanias et al. [10] show that the additional value of EMG signals is marginal for an adaptive model compared to a non-adaptive model.

1) Echo control: With this control scheme, the prosthetic limb is controlled such that it will mimic the kinematics of the previous cycle of the unaffected leg. This scheme is then individualized and responds to the cadence of the user. It also can deal with different locomotion modes, because it simply mimics the movement of the other leg [5], [12]

This control scheme is based on the assumption that the unaffected limb inputs a desirable input trajectory. However, this might not be the case. As is mentioned in section A-A1, pathological gait is not symmetric. [12] Another problem could be if the user missteps: this will be imitated by the prosthesis and can result in safety issues. For example, if the user stumbles with the healthy leg, the prosthesis will mimic this behavior.

Furthermore, additional instrumentation on the unaffected leg is necessary. This restricts the use of the prosthesis to unilateral amputees and also results in problems for an odd number of steps: The prosthesis will always move one step if the biological leg does so. To change the locomotion mode, the biological leg must be in front. [5], [12] Furthermore, additional sensors should be applied to the biological limb to mimic its behavior.

The advantages of individualization and response to cadence do not outweigh the disadvantages and risks.

2) Rule-based detection: Currently, manual mode switching schemes are implemented in many applications due to simplicity and reliability. [15] This means, for instance, that the user pushes a button and the devices switches between modes. There is no available automatic gait mode recognition scheme that is capable of reliably detecting all modes in real-time and using a minimalist sensor array [15]. However, several approaches have been taken. These methods use a rule-based system: the designer defines the possible gait modes and identifies a fixed set of rules that indicate the transition between different modes. These rules may be based on the sensed state of the user, device or the environment at a given point in the gait cycle.[1]

These rules evaluate the value of different parameters, criteria might be selected manually or through analytical means [1]. For example, Grimes [12] used the knee angle at foot contact. If this angle is larger than 62 degrees, stair ascent is recognized. In case the knee angle is smaller than 30 degrees, walking is recognized. This is always one step too late: the foot is already on the stairs before the knee angle crosses the threshold.

Parri et al. [13] use a combination of ground reaction forces, joint angles of knee and hip and angular velocities of the thighs, shanks, and feet. Since the algorithm needs the information on both sides, IMUs are placed on the chest, thighs, shanks, and feet.

Li et al. [15] used the vertical position of the IMU and the pitch angle of the foot to recognize stair ascent. However, this algorithm compares the orientation and position to a threshold. This means that the threshold is only crossed if the subject is already standing on the stairs, and therefore does not recognize the transition itself.

Jang et al. [14] use a Fuzzy inference system to differentiate between the different walking modes. For their system, they use the hip angle and the absolute difference between the hip angles. However, this means that they need information about both hip angles.

To conclude, different parameters have been used, but often in combination with additional equipment.

3) Detection by machine learning: The clear benefit of using an automated classifier over one based on heuristic rules is that data from a multitude of sensors can be input to the classifier, from which additional features may be computed and used to make classification decisions that are less biased and potentially more accurate due to the high-dimensional input. Manual identification of these decision boundaries would likely be intractable otherwise [1].

Previous research has shown that machine learning algorithms can be used for intention detection. An overview of the used methods and products can be seen in TABLE IV. It can be seen that different prostheses have been used, which come with different sensors in the prosthesis. Furthermore, different classifiers have been used. Huang et al [16] recommend using an LDA. It results in accuracies comparable to an ANN, but needs a shorter time for training, is easy to design, and computationally efficient for real-time prosthesis control [16]. However, this method focuses on surface EMG instead of using mechanical sensor information. Furthermore, a support vector machine (SVM) also seems promising.

C. Machine learning approach

A few terms are important for the performance of the algorithms. First, the bias: this represents the simplifying assumptions that have been made by a model to make the target function easier to learn. [23] A low bias results in more assumptions about the form of the target function, while high bias results in fewer assumptions about the form of the target function. High bias results in a fast-learning model and it is easy to understand the model. However, it is less flexible [23] Variance is the amount that the estimate of the target function will change if a different training set was used. Low variance suggests small changes to the estimate of the target function with changes to the training dataset. High variance suggests large changes to the estimate of the target function with changes to the training data set. [23]
It is important to note that there is a relationship between the variance and the bias: increasing the bias will decrease the variance and vice versa. [23]
Another trade-off is the fitting of the data. Overfitting results in a good performance on the training data, but a poor generalization on other data. Underfitting results in poor performance on the training data and a good generalization of other data. This problem can be solved by resampling methods or a validation data set. [23]

1) Linear Discriminant Analysis (LDA): Linear Discriminant Analysis (LDA) can be used for dimensionality reduction. It is comparable to Principal Component Analysis (PCA), but instead of only focusing on the largest amount of variance, it also considers the labels of the class. This results in being able to select the features with the largest differences between classes. [24]

Equation (4) calculates the within scatter matrix, which represents the amount of scattering within the class. Equation (6) calculates the between-scatter matrix, which represents the amount of scattering between classes. The bigger the ratio between these two is, the easier to separate between the classes. Therefore, the eigenvector of $S_W^{-1} S_B$ is calculated. [25] Fig. 17 shows the different scenarios with respect to the separability between the different classes.

$$S_W = \sum_{i=1}^{c} S_i \tag{4}$$

$$S_i = \sum_{x \in D_i}^{n} (\mathbf{x} - \mathbf{m}_i)(\mathbf{x} - \mathbf{m}_i)^{\mathrm{T}} \tag{5}$$

$$S_B = \sum_{i=1}^{c} n_i (\mathbf{m}_i - \mathbf{m})(\mathbf{m}_i - \mathbf{m})^{\mathrm{T}} \tag{6}$$

$$\mathbf{m}_i = \frac{1}{n_i} \sum_{x \in D_i}^{n} \mathbf{x}_k \tag{7}$$

With
n_i Sample size for respective class
$\mathbf{m}_i$ Mean vector of all features for respective class
$\mathbf{m}$ Mean vector of all classes

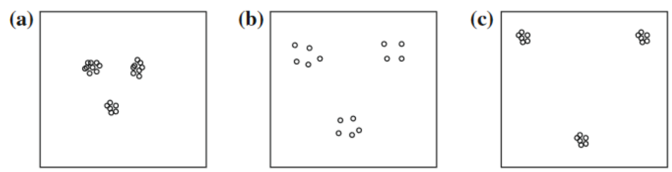

Fig. 17: (a) Classes with a small between-class distance and small within-class variance. (b) Classes with small between-class distance and large within-class variance. (c) Classes with large between-class distance and small within-class variance. [26]

The related eigenvalues are then sorted based on decreasing value: the bigger the value, the larger amount of variance this feature explains. By calculating the relative amount of the variance it explains, the most important features can be determined [27]. These features can then be transformed into the the new feature space using equation (8).

$$\mathbf{Y} = \mathbf{X} \times \mathbf{W} \tag{8}$$

With
$\mathbf{Y}$ The transformed data
$\mathbf{X}$ The original data
$\mathbf{W}$ Eigenvectors of the used features

2) Support Vector Machine (SVM): An SVM is a decision machine, and will therefore not provide probabilities. It decides whether a data point is part of a class based on a model. equation (9) shows the equation for a linear model, in which $\phi(\mathbf{x})$ denotes a fixed feature-space transformation, b is an explicit bias parameter. For this linear model, the assumption is made that the training data set is linearly separable in feature space. Other options, such as a Gaussian or polynomial kernel are also possible.
An SVM is more computationally efficient than other non-linear classifiers such as an Artificial Neural Network (ANN) [4]. Furthermore, the trade-off between the bias and the variance can be tuned manually by changing the C-parameter, which influences the number of violations of the margin is allowed in the training data. [23]

$$y(\mathbf{x}) = \mathbf{w}^T \phi(\mathbf{x}) + b \tag{9}$$

TABLE IV: Overview of prostheses and their used parameters and classifications

Research group	Prosthesis	Features	Classifier	Hyperparameters
Cooperation between institutions [5], [4]	Able-bodied: Walking shoes Amputees: Own prosthesis	EMG signals (mean abs, # of zero crossings, # of slope sign changes, waveform length) 6 DOF load cell (mean, min, max)	SVM	Nonlinear kernel (RBF) One-against-one Majority voting
University of Rhode Island [16], [7], [8]	Able-bodied: Walking shoes Amputees: Own prosthesis	EMG signal, time-domain features (mean abs, # of zero crossings, # of slope sign changes, waveform length) EMG signal, auto regression features (features with three-order auto-regression coefficients and root mean square of a signal)	LDA	
University of Rhode Island [16]	Able-bodied: Walking shoes Amputees: Own prosthesis	EMG signal, time-domain features (mean abs, # of zero crossings, # of slope sign changes, waveform length) EMG signal, auto regression features (features with three-order auto-regression coefficients and root mean square of a signal)	ANN	Fully connected two-layer ANN Training: standard back-propagation 10 hidden units
Center for Bionic Medicine [9]	VanDerBilt prosthesis (knee and ankle)[28], [29]	Accelerometer and gyroscope on socket, two pressure sensors under shoe sole (ball flat and heel)(mean, sd, min, max)	LDA	
Human Neuromechanics Laboratory [30], [18], [31]	VanDerBilt prosthesis (knee and ankle)	Potentiometers and encoders at knee and ankle, axial load cell, six-axis IMU on shank. Knee and ankle positions, velocity and torque, axial force, shank three-directional accelerations and rotational velocities. (mean, sd, min, max, initial, final)	DBN	
Center for Bionic Medicine [31]	VanDerBilt prosthesis (knee and ankle)	relative knee and ankle positions, velocities, and commanded joint torques. 6DOF load cell, 6DOF IMU, thigh angle, shank angle (mean, sd, min, max, initial, final)	ANN	One hidden layer, 20 hidden neurons training: scaled conjugate gradient learning algorithm and hyperbolic tangent activation function
VanDerBilt University [32], [3]	VanderBilt Prosthesis	Joint angles, angular velocities of the prosthesis joints, interaction forces and torques between user and prosthesis, interaction forces and torques between prosthesis and environment. Acceleration and EMG measurements from residual limb. (Mean and standard deviation, normalized)	GMM	
VanderBilt University [10]	VanderBilt prosthesis [33]	8 EMG channels, abs value, waveform length, zero crossing, slope sign changes, autoregressive coefficients of model Knee and ankle joint kinematics, motor currents, calculated thigh and shank inclination angles, 6DOF forces and moments (mean, sd, min, max, initial, final)	DBN Adaptive	